Orientational Order in Strained Nematic Networks

P. Bladon, M. Warner, and E. M. Terentjev*

Cavendish Laboratory, Madingley Road, Cambridge CB3 0HE, U.K.

Received May 2, 1994; Revised Manuscript Received July 26, 1994®

ABSTRACT: Monodomain nematic networks, formed by cross-linking polymer liquid crystals in ordered states, retain a memory of their anisotropic cross-linking conditions and thereby show novel elasticity and strain-induced nematic transitions. Up to a certain critical strain the nematic director can experience a barrier to its rotation. Orientational transitions can result, and these are investigated using a simple model of nematic elastomers that allows both the direction and the magnitude of order to respond to applied strains. We find two temperature dependent regimes. At low temperatures where nematic effects are strong, the director rotates the switches with the nematic order largely intact. At higher temperatures near the thermodynamic phase transition elastic effects dominate and applied strain destroys the nematic order before it re-forms in the new direction. This corresponds to the two regimes found experimentally.

1. Introduction

Polymer liquid crystals (PLC's) are long-chain macromolecules which, due to a combination of intermolecular orientational interactions and intrinsic stiffness, can orientationally order at low temperatures into a nematic phase in which the polymer adopts a prolate or oblate conformation, with the polymer backbone preferring to align along or normal to an ordering direction **n**, the director.

Nematic rubber, created by cross-linking PLC's, has many new and unusual properties. At and below the nematic–isotropic (NI) transition, PLC molecules spontaneously change their shape with temperature. Cross-linking PLC's to form a rubber allows these molecular shape changes to couple to macroscopic deformations of the network. This gives rise to the unusual properties of nematic rubber, first predicted by de Gennes.[1] The coupling of nematic ordering to strain can give rise to a spontaneous shape change at the nematic–isotropic (NI) transition, nonlinear and discontinuous stress–strain relationships, a mechanical critical point, and changes in the NI transition temperature.

Subsequent experiments have seen the basic effects predicted by de Gennes: shifts in the transition temperature with cross-linking density and state (nematic or isotropic) and unusual stress–strain relations in the region of the NI transition.[2] However, networks cross-linked in the isotropic phase form polydomain nematic networks in which many of the networks properties are masked. In order to do optical experiments on PLC's it is necessary to produce a macroscopically uniform sample. Such uniformity can be produced by straining the material to align all the microdomains. However as the strain is released, the material recovers its original structure.

More recently, new techniques have evolved to produce monodomain or "single crystal" nematic networks. The theoretical study of monodomain nematic networks presented in this paper is motivated by two beautiful papers describing strain experiments on monodomains[3,4] formed by two different routes. The samples of Küpfer and Finkelmann[3] were formed by a two-step cross-linking process. The PLC was cross-linked once, stretched to achieve a uniformly oriented sample, and cross-linked again in this ordered state. Mitchell *et al.*[4,5] cross-linked PLC in an ordered state produced by the application of a magnetic field. Cross-linking in an ordered phase gives the material a memory of the cross-linking direction and magnitude. Experiments by Legge *et al.*[5] show that repeated heating and cooling does not destroy the direction, **n**, or magnitude, Q, of this order.

Both groups performed experiments on a sheet of rubber containing a director aligned parallel to the surface. The sheet was strained at an angle perpendicular to this director, to see how the magnitude and direction of order varied. Both found the director rotating to align itself with the strain direction, sometimes via an orientational phase transition. Küpfer and Finkelmann have measured the order parameter in the initial and final states; Mitchell *et al.* were able to measure the evolution of Q and the direction of the nematic director **n** as strain was increased. Küpfer *et al.* found that after realignment the order had decreased (Q moving from $0.56 \rightarrow 0.36$) and that at an intermediate strain the order had been lost entirely, the sample reverting to the scattering state. Mitchell *et al.* found that although the magnitude of order was reduced in the vicinity of the transition, on further strain it returned to nearly its initial value. Mitchell *et al.* were able to identify the location of the transition unambiguously by following the discontinuous jump in the direction of order in the network.

In this paper we explore the differences between these two apparently contradictory results by studying the simplest possible microscopic model for these systems, namely a model of nematic rubber elasticity involving anisotropic Gaussian statistics, including a self-consistent model for PLC chains that underly this anisotropy. We shall concentrate on the simple geometry used in experiments thus far, where shear strains are suppressed. For a discussion of instabilities in other geometries we refer the reader to ref 6.

Earlier microscopic theories of nematic networks mainly dealt with networks formed in an isotropic state.[7-10] These theories display the qualitative behavior seen in earlier experiments. Recent theory[6] for the elastic part of the free energy, essentially treats an anisotropic, monodomain Gaussian rubber and predicts a rich variety of orientational transitions, where the resistance to rotation of the nematic director is subtly dependent on mechanical constraints applied to the sample. In particular, a strain applied perpendicular to the memory direction is resisted by a barrier to director rotation, resulting in a transition of the director (perhaps reminiscent of Fredericks[11]), which has been recently seen experimentally.[4] The transition is driven by surface fields (the applied stresses) which are

® Abstract published in *Advance ACS Abstracts*, September 15, 1994.

0024-9297/94/2227-7067$04.50/0

resisted by a bulk barrier to rotation (the memory anisotropy). This is in fact the opposite of a conventional Fredericks transition which is driven by a bulk field (the EM field) and resisted by surface barriers to rotation. The theory has also explained[12] some apparently contradictory results of applying electric fields to nematic rubbers, and a whole new class of "soft" deformations.[13,14] Soft modes of deformatin occur when certain combinations of the elements of the strain tensor are involved. Along with this particular class of strain is a rotation of the director but *no* increase in the free energy; that is, ideally the strain can occur without the application of stress. This has also been predicted on general grounds of continuum symmetry by Golubovic and Lubensky.[15] The freedom of the director to perform these special rotations without cost of energy does not mean there is no nematic memory cross-linked in. This favored set of distortions is a small manifold of all those available and it depends critically upon the initial state.

In the theoretical papers cited above, the transitions were predicted by assuming that the *magnitude* of the nematic order is decoupled from the elastic free energy, only its *direction* responding to applied strains. This allowed simple analysis of the free energy, and in some cases (where all components of the strain are entirely fixed) allows the director transitions to be predicted exactly. For cases where one strain is applied and the other strain components are allowed to relax (as happens more typically in an experiment), the strain relaxation couples to the nematic free energy of the system. At low temperatures where there is a high degree of ordering, changes in the magnitude of nematic order under strain should be small. At such temperatures, or when the deformation is soft, the nematic and elastic free energy should effectively only couple through the direction of ordering. However, this should not necessarily be the case at higher temperatures, when the nematic order is not so rigidly set.

When the magnitude of the order can change as well as the direction, one needs to apply a particular molecular model for the nematic PLC. We choose to use the freely jointed rod model. In subsequent sections we summarize the theory of anisotropic Gaussian elasticity of networks and review the relevant results for the experimental geometry of Mitchell *et al.* and Küpfer *et al.* In section 2 we revisit the freely jointed rod model of a nematic polymer. We discuss the free energy of the nematic rubber and effects of its spontaneous relaxation with changing temperature. In section 3 the two halves of the theory, for the ordering and for the elasticity, are coupled together and numerical results are presented. We consider two qualitatively different situations—when the sample is strained at very low temperatures and when an experiment is performed near the nematic–isotropic transition point. We show that in the latter case the nematic network undergoes a sequence of two ordering transitions along with orientational switching.

1.1. Elastic Free Energy. In this section we summarize the concepts, leading to the elastic free energy of a nematic network, and discuss the relevant results for the geometry used in the strain experiments.

One of the characteristics of a polymer liquid crystal molecule is that its chain conformation in a nematic phase is anisotropic. If an isolated nematic chain is long, the chain statistics will be Gaussian, albeit anisotropic. Furthermore at melt densities we also expect that the screening of excluded volume interactions will result in a collection of such chains also having Gaussian statistics. Assuming that PLC chains behave as noninteracting anisotropic Gaussian coils allows us to generalize classical elasticity theory to the case of anisotropic coils, as described in ref 6.

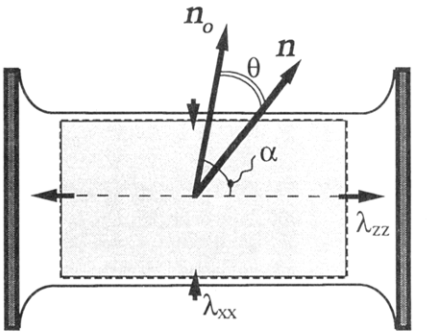

Figure 1. Experimental geometry. Deformation λ_{zz} is applied at an angle α to the initial director $\mathbf{n}^0$. There is a shrinkage λ_{xx}, $\lambda_{yy} < 1$ in the transverse directions x (shown) and y. The current director, $\mathbf{n}$, is shown rotated by an angle θ from its original direction.

We describe the network by a Gaussian distribution $P[\mathbf{R}]$ of chain end-to-end vectors, $\mathbf{R}$. Using a superscript ^{0} to denote quantities at the initial state before applying the strain, the mean square end-to-end distance of a network chain is given by $\langle R_i^0 R_j^0 \rangle = {}^1/_3 L l_{ij}^0$, where L is the chain contour length and l_{ij}^0 defines the effective step lengths of the Gaussian, uniaxially anisotropic random walk at cross-linking. In its diagonal frame this matrix has two distinct components which we denote $l_\parallel^0$ and $l_\perp^0$, describing the step length parallel and perpendicular to the uniaxial director at cross-linking. As the network deforms, the step length tensor alters to a new l_{ij}, with diagonal elements which we label $l_\parallel$, l_1, and l_2, distinguishing now between the two perpendicular components ($l_\parallel^0 \rightarrow l_\parallel$; $l_\perp^0 \rightarrow l_1$, l_2) since the chain conformation may become biaxial. When the affine deformation assumption is employed, an assumption that pervades network theory, junction points move affinely from their original positions with the bulk deformation $R_i = \lambda_{ij} R_j^0$. λ_{ij} is the uniform strain tensor that describes a deformation. Using this assumption, the elastic free energy per network strand is, in units of $k_B T$

$$\frac{F_{el}}{k_B T} = \frac{1}{2}\left[Tr[\underline{\underline{l}}^0 \cdot \underline{\underline{\lambda}}^T \cdot \underline{\underline{l}}^{-1} \cdot \underline{\underline{\lambda}}] - \ln\left(\frac{\mathrm{Det}[\underline{\underline{l}}^0]}{\mathrm{Det}[\underline{\underline{l}}]}\right)\right] \qquad (1)$$

Since the shear modulus of rubber is around 10^6 N/m^2 and the modulus for volume change is typically 10^{10} N/m^2, deformations of elastomers are at constant volume (to within 10^{-4} accuracy), that is $\mathrm{Det}[\lambda_{ij}] = 1$.

The various step lengths of the anisotropic l_{ij} depend on the nematic order parameter Q_{ij}, the dependence being determined by the choice of model for the PLC. The elastic free energy therefore depends on the state of order at formation, Q_{ij}^0, through l_{ij}^0, and upon the current state of order Q_{ij}, through l_{ij}. In turn Q_{ij} will depend implicitly upon λ_{ij}. It is the purpose of this paper to investigate how Q_{ij} changes self-consistently in both magnitude and direction, affecting the elasticity of a nematic rubber.

In order to make the above free energy correspond to an experimental system we must specify the coordinate systems and components of (1). We look only at the geometry described in Figure 1, that was used in the experiments of Mitchell *et al.*[4,5] and Küpfer *et al.*[3] above. Each end of a flat sample is clamped and the ends are pulled apart, fixing the extension magnitude $\lambda_{zz} = \lambda$. The clamping prevents any shear deformations, hence $\lambda_{xz} =$

$\lambda_{zz} = 0$ everywhere in the sample (except, perhaps, small nonuniform areas near the clamps). The transverse dimensions λ_{xx} and λ_{yy} are allowed to relax to the values that minimize the free energy, subject to the incompressibility constraint, $\mathrm{Det}[\lambda_{ij}] = \lambda\lambda_{xx}\lambda_{yy} = 1$. The cross-linking fixes the director $\mathbf{n}^0$; we choose the sample to be oriented so that $\mathbf{n}^0$ is in the $(\hat{z}, \hat{x})$ plane, at an angle α to the stretching direction $\hat{z}$. Stretching will cause the director $\mathbf{n}$ to rotate through an angle θ in the $(\hat{z}, \hat{x})$ plane around the $\hat{y}$ axis. All calculations of the components of l_{ij} and Q_{ij} will be performed in the coordinate system in which Q_{ij} (and hence l_{ij}) is diagonal. These diagonal tensors will then be rotated through some (as yet undetermined) angle $\Delta = \alpha - \theta$ so that all quantities are expressed in the same Cartesian coordinate system as the deformation tensor λ_{ij}, Figure 1. Since all rotations taken place in the $(\hat{z}, \hat{x})$ plane, it is sufficient to consider all matrices to be (2×2).

With this geometry, the elastic free energy per network strand is

$$\frac{F_{el}}{k_B T} = \frac{1}{2}\left[ad\lambda^2 + be\lambda_{xx}^2 + 2cf\lambda\lambda_{xx} + \frac{r}{\lambda_{xx}^2\lambda^2} - \ln\left(r\frac{\mathrm{Det}[l^0]}{\mathrm{Det}[l]} \right) \right] \quad (2)$$

The coefficients a–f arise from writing $l^0 = \begin{pmatrix} a & c \\ c & b \end{pmatrix}$ and $l^{-1} = \begin{pmatrix} d & f \\ f & e \end{pmatrix}$ and depend on the angles α and Δ. Defining the mean and anisotropy of the tensors l_{ij}^0 and l_{ij}^{-1} to be $\overline{l^0} = (l_\parallel^0 + l_\perp^0)/2$, $\delta l^0 = (l_\parallel^0 - l_\perp^0)/2$, $\overline{l^{-1}} = (l_\parallel^{-1} + l_1^{-1})/2$, and $\delta l^{-1} = (l_\parallel^{-1} - l_1^{-1})/2$, respectively, we have

$$\begin{aligned} a &= \overline{l^0} + \delta l^0 \cos 2\alpha & b &= \overline{l^0} - \delta l^0 \cos 2\alpha \\ c &= -\delta l^0 \sin 2\alpha & d &= \overline{l^{-1}} + \delta l^{-1} \cos 2\Delta \\ e &= \overline{l^{-1}} - \delta l^{-1} \cos 2\Delta & f &= -\delta l^{-1} \sin 2\Delta \\ r &= l_\perp^0 / l_2 \end{aligned} \quad (3)$$

The strain λ_{yy} has been written as $1/\lambda\lambda_{xx}$ in the fourth term of (2) according to the incompressibility constraint.

The free energy must be minimized with respect to the remaining free strain component λ_{xx} and the three variables specifying the state of order, θ, which sets the diagonal frame for Q_{ij} (*i.e.* the angle that $\mathbf{n}$ makes with $\mathbf{n}^0$), and the two scalar order parameters Q and X describing the magnitude of uniaxial and biaxial order in that frame. Equating the partial derivative of (2) with respect to λ_{xx} to zero results in an algebraic equation which can be solved for λ_{xx}:

$$be\lambda_{xx}^4 + cf\lambda_{xx}^3 - \frac{r}{\lambda^2} = 0 \quad (4)$$

When $\alpha = \pi/2$, i.e. the stretching direction is perpendicular to the initial uniaxial anisotropy $\mathbf{n}^0$, the elastic free energy is particularly simple, as the coefficient c in (2)–(4) is equal to zero. The values of λ_{xx} and λ_{yy} which minimize the free energy are given by

$$\lambda_{xx} = \left(\frac{r}{be}\right)^{1/4} \frac{1}{\lambda^{1/2}} \qquad \lambda_{yy} = \left(\frac{be}{r}\right)^{1/4} \frac{1}{\lambda^{1/2}} \quad (5)$$

Inserting these values into (2) yields the free energy as a function of θ, Q^0, and Q only [through the coefficients in (3)]

$$\frac{F_{el}}{k_B T} = \frac{1}{2}\left[ad\lambda^2 + 2\frac{(rbe)^{1/2}}{\lambda} - \ln\left(r\frac{\mathrm{Det}[l^0]}{\mathrm{Det}[l]} \right) \right] \quad (6)$$

The final state of strain is not uniaxial. The free energy (6) has either three extreme points in θ, minima at $\theta = 0$ and $\pi/2$ with a maximum in between, or two extreme points, a minimum at $\theta = 0$ and a maximum at $\pi/2$, or vice versa. Which situation occurs depends on the magnitude of the imposed deformation λ. We can identify three points, the limit of stability, $\lambda_{c'}$, of the solution with an undistorted director ($\theta = 0$), the limit of stability of the solution with $\theta = \pi/2$ (full director rotation) denoted by $\lambda_{c''}$, and the point at which the free energies of the two solutions become equal (thermodynamic transition point) which we will denote by λ^*. The values of extension at these points are given by

$$\lambda_{c'}^3 = \left(\frac{l_\parallel^0 l_\parallel}{l_\perp^0 l_2}\right)^{1/2} \qquad \lambda_{c''}^3 = \left(\frac{l_\parallel^0 l_1}{l_\perp^0 l_2}\right)^{1/2} \quad (7)$$

$$(\lambda^*)^3 = \left(\frac{l_\parallel^0 l_\parallel l_1}{l_\perp^0}\right)^{1/2} \frac{1}{l_\parallel^{1/2} + l_1^{1/2}} \quad (8)$$

One sees, naturally, that $\lambda_{c''} < \lambda^* < \lambda_{c'}$. These values of λ set the bounds for any hysteresis present in the orientational transition under strain. In network systems hysteresis effects could be significant. The size of the thermal fluctuations, $\sim k_B T$, is very much less than the size of the macroscopic free energy barrier that must be overcome to achieve a phase transition $\sim n_s k_B T$, with n_s of the order of the number of elastically active network strands in the system. Mechanisms such as nucleation which would allow the system to get around the transition barrier are probably suppressed in a cross-linked system. Nematic rubbers could therefore become trapped in metastable phases due to macroscopic barriers which prevent them from attaining their global minimum free energy. Upon stretching, the director would then remain undistorted at $\mathbf{n}^0$ ($\theta = 0$) past the thermodynamic transition point $\lambda = \lambda^*$, until the metastable state becomes totally unstable at $\lambda = \lambda_{c'}$, whereupon θ jumps to $\pi/2$. On reducing the strain λ back toward its starting value, the nematic director remains at its rotated position $\theta = \pi/2$ until this phase becomes unstable at a $\lambda = \lambda_{c''}$, whereupon the director returns to θ equals zero.

1.2. Summary of Results for a Fixed Magnitude of Order. In the previous work the variation of the magnitude, Q, of Q_{ij} was ignored but $\mathbf{n}$ was allowed to vary (*i.e.* l_{ij} was considered to be simply a rotated version of l_{ij}^0). This allows simple analysis as all the physics is then contained in the elastic free energy, the nematic free energy being constant. The assumption relates to low temperatures where the order is high and changes direction rather than amplitude. When the magnitude of Q is held constant at Q^0, l is merely a rotated version of l^0 and hence $l_\parallel = l_\parallel^0$, $l_1 = l_2 = l_\perp^0$, and $r = 1$. The two free energies (6) are

$$\frac{F_{el}}{k_B T} = \begin{cases} \frac{1}{2}\left[\lambda^2 + \frac{2}{\lambda}\right] & \text{for } \theta = 0 \\ \frac{1}{2}\left[\left(\frac{\lambda}{\lambda_o}\right)^2 + 2\left(\frac{\lambda_o}{\lambda}\right)\right] & \text{for } \theta = \pi/2 \end{cases} \quad (9)$$

with $\lambda_o = (l_\parallel^0 / l_\perp^0)^{1/2}$.

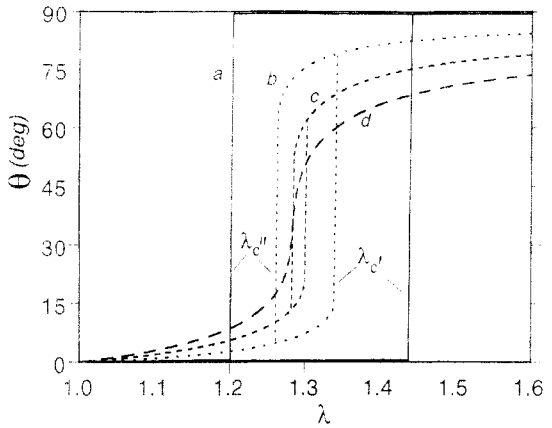

Figure 2. Rotation, θ, of the director against imposed strain λ in the z direction for various angles α between z and the original director: (a) $\alpha = 90°$; (b) $\alpha = 87.5°$; (c) $\alpha = 85°$; (d) $\alpha = 82.5°$. The initial anisotropy of the PLC is $l_\parallel^0/l_\perp^0 = 3$. For $\alpha > \alpha_c$ there are discontinuous jumps of θ with λ. The upward jump occurs at $\lambda_{c'}$ and the downward jump, as strain is reduced, at $\lambda_{c''}$. There is a region of hysteresis between them. The magnitude of the nematic order is approximated as frozen as the strain increases, the response of the system being limited to the rotation of the order.

When $\theta = 0$, the nematic director is not rotated and the free energy is that of a classical Gaussian elastomer. When $\theta = \pi/2$ (after the anisotropy axis has been aligned along the strain direction), the free energy is again like that of a classical Gaussian elastomer but with a different natural shape λ_0. When the angle of application of strain $\alpha \neq \pi/2$, minimizing the free energy numerically with respect to θ results in the curves for the director orientation θ as a function of λ summarized in Figure 2.

Discontinuous transitions persist for values of $\alpha \neq \pi/2$, *i.e* when the extension is at an oblique angle to the initial nematic director. The presence of discontinuous transitions is a result of the internal barrier to rotation, not of a degeneracy at exactly $\alpha = \pi/2$. With the assumption that the magnitude of Q is constant, all the transitions summarized in Figure 2 depend *only* on the initial anisotropy, in fact only on the measurable quantity $\lambda_c = (l_\parallel^0/l_\perp^0)^{1/3}$, and the sample shape change on cooling from an isotropic state,[7,8] and not on any other parameters. The extent to which this prediction remains valid when the magnitude of order is allowed to change is a major concern of this paper.

1.3. The True Stress. The true stress (true stress = force/current area) required to produce the above deformations is, when f is the free energy per unit volume,

$$\sigma = \lambda \frac{\mathrm{d}f}{\mathrm{d}\lambda}\Big|_\lambda \tag{10}$$

For $\alpha \approx \pi/2$, when the extension axis is close to perpendicular to the initial anisotropy axis, the $\theta = 0$ phase becomes unstable at $\lambda_{c'}$ and the free energy drops down to the lower branch associated with the large θ ($\approx\alpha$) phase. It turns out (we show qualitatively similar free energy plots later) that the minimum of this branch of F_{el} occurs at still higher values of λ and hence the slope $\partial F_{el}/\partial\lambda$ is negative. Thus the stress is negative at this point. The physical consequences of negative stress depend on how the experiment is being done. If the *strain* is fixed, as the transition occurs the network will want to spontaneously elongate. Depending on the sample's shape, it could buckle. If the *stress* is being held constant, at the transition point there will be a spontaneous shape change. Likewise the transition back to the small θ state occurs at a negative stress. One would have to compress the sample to recover the initial state. After the sample is stretched and one end is unclamped, the rubber is very slow to recover its initial state. Similarly, returning the apparatus to $\lambda = 1$ results in a buckling of the sample. The only quick way to fully recover the initial state is to heat the sample above its nematic–isotropic transition temperature. We would conclude therefore that the existence of negative stress regions and hysteresis are consistent with the experimental observations of Mitchell.

The systems used in experiments of Finkelmann *et al.*[2,3] seem to be fundamentally different from the monodomain systems we have described so far. Polymer chains are initially weakly cross-linked in the isotropic phase, thereby recording a polydomain structure in the sample. [The polydomain structure becomes visible by cooling the once-cross-linked system to the nematic phase.] When a uniaxial stress is applied, the material is cross-linked a second time. The internal stresses thereby created evidently lead to a nematic monodomain on cooling. In effect each domain, initially misaligned, is forced to conform by the imposed strain. In this process, however, the local magnitude of order in each domain may become quite nonuniform and the fact that finite stresses are required to convert a once-cross-linked nematic polydomain elastomer into a monodomain suggests a possible interaction of domains even once aligned.

2. Self-Consistent Nematic Order in a Strained Network

In this section we remove the assumption of the constancy of the uniaxial order parameter, $Q = Q^0$, $X = 0$. We discuss a model for polymer liquid crystals that gives explicit relations between step lengths l and the order parameters Q and X which allow us to apply a self-consistent procedure to determine these parameters as functions of an applied strain. We then generalize to the case of the elastic free energy where the experimental temperature is lower than that of the cross-linking.

2.1. Freely Jointed Rod Model of a PLC. Thus far, to make predictions of experimental behavior, it has been necessary to make an assumption about the behavior of the order parameter, namely that it remains constant in magnitude. Our description was thus model independent, using only a single (observable) parameter $\lambda_c = (l_\parallel^0/l_\perp^0)^{1/3}$. In order to investigate the effect of a varying Q we need a specific model for the nematic free energy of a PLC.

Most nematic networks, including those synthesized by Davies *et al.*[16] and Finkelmann *et al.*,[17] are formed from side chain PLC's, although some backbone systems have also been made.[18] We therefore need a model of PLC's that replicates side chain behavior. The most important factor governing the behavior of a side chain PLC is the nature of the molecular "hinge" joining the side to main chains.[19-21] If this hinge group is short and consists of an even number of CH_2 groups, the backbone is forced to lie perpendicular to the side chains and adopts an oblate spheroidal shape. If a network is formed from such polymers the stress-optical coefficient is negative. If the hinge group is long, or has an odd number of CH_2 units, then the main and side chains prefer parallel alignment, resulting in a positive stress-optical coefficient. The experimental results that we shall discuss relate to side chain PLC's that have this particular coupling. There have been several theories of side chain liquid crystals, some assuming "negative" coupling,[22] others leaving the sign of the coupling as a parameter in the theory.[23-25] The

main observation is that, in the absence of any intrinsic backbone nematicity, the backbone becomes weakly coupled to the side chain order parameter. Explicitly, one could construct a theory by following Warner *et al.*,[24,25] coupling Maier–Saupe-like side chains to a backbone chain, letting the coupling become weak, and solving for the backbone order as a function of side chain order. This approach introduces a new parameter (the side chain–main chain "hinge" coupling) without introducing any new physics. In order to avoid complicating the theory unnecessarily we choose to use the freely jointed rod model of a PLC, which has the same symmetry as the real system *i.e.* increasing order increases the chain anisotropy weakly in the ordering direction. In the freely jointed rod model the coupling of the order to the chain shape is weak, as is the case for real side chain systems. This model was first used for nematic chains in the network context by Abramchuk and Khokhlov.[7]

We model a PLC as a freely jointed chain of Maier–Saupe rods. Pairs of cylindrically symmetric rods are taken to interact via a quadrupolar potential $U(\Phi) = -\upsilon P_2(\cos\Phi) \equiv -\upsilon(3\cos^2\Phi - 1)/2$ of intrinsic uniaxial symmetry (Φ is the angle between the two rods). Replacing this pair interaction by an interaction between one molecule and a spatially uniform mean field with major axis in the $\hat{z}$ direction gives

$$Z = \int_0^{2\pi}\int_{-1}^{1} du\, d\phi \exp(-\beta U(u,\phi)) \tag{11}$$

$$U(u,\phi) = -\upsilon Q P_2(u) - \frac{\upsilon X}{2}(1-u^2)\cos 2\phi \tag{12}$$

$$Q = \langle P_2(u)\rangle \qquad X = \frac{3}{2}\langle(1-u^2)\cos 2\phi\rangle \tag{13}$$

where $u = \cos\theta$ with θ the angle of a rod with the $\hat{z}$ direction (polar angle) and ϕ the azimuthal angle in the corresponding spherical coordinate system. Q is the uniaxial order parameter; X, the degree of biaxiality. The nematic free energy per rod of the chain is then

$$\frac{F_{nem}}{k_B T} = -\log Z + \frac{\beta\upsilon Q^2}{2} + \frac{\beta\upsilon X^2}{6} \tag{14}$$

The extra two terms in the free energy arise from the need to eliminate the double counting introduced by the mean field and are necessary for self-consistency. Although the theory of Maier and Saupe permits a biaxial order parameter, in the absence of external fields the minimum of (14) only permits uniaxial solutions. For real biaxiality to arise with uniaxial molecules, external fields such as those provided by stressing a nematic network, are required. For a melt of freely jointed rod chains of the Maier–Saupe type, there is a phase transition at a reduced temperature $\tilde{T} \equiv k_B T/\upsilon = 0.2202$ to a value of the order parameter $Q = 0.4290$ with $X = 0$.

Since successive chain segments are uncorrelated, the freely jointed chain has Gaussian statistics, with $\langle R_i^2\rangle = {}^1/_3 L l_i$. The effective step lengths are given by

$$l_\parallel = l_o(1+2Q) \qquad l_1 = l_o(1-Q+X) \qquad l_2 = l_o(1-Q-X) \tag{15}$$

Uniaxial orientation causes the chain to adopt a prolate ellipsoid configuration. The maximum increase in chain length going from an isotropic state ($Q = 0$) to a completely ordered state ($Q = 1$) results in a change in $l_\parallel$ of a factor of 3. This does not allow freely jointed rod PLC's access to a regime where they become rodlike or highly extended, as can happen in experimental main chain systems, see ref 26. However, where the coupling between ordering and chain shape is weak, as one expects in a side chain system, one perhaps expects the freely jointed rod model to describe the variation in the step lengths with Q better than an equivalent wormlike chain theory in which the coupling is strong.

2.2. Free Energy of a Nematic Network. When mechanical experiments are conducted at a different (normally lower) temperature from that at which the cross-linking has been performed, $T \neq T_X$, then the rubber relaxes macroscopically before strains are applied. In practice strains are measured with respect to this modified state.

The free energy of a nematic network of Gaussian chains interacting via a nematic mean field is

$$F = n_s F_{el} + n_s N F_{nem} \tag{16}$$

or

$$\frac{F}{n_s k_B T} = \frac{1}{2}\left[Tr[\underline{\underline{l}}^0\cdot\underline{\underline{\lambda}}^T\cdot\underline{\underline{l}}^{-1}\cdot\underline{\underline{\lambda}}] - \ln\left(\frac{\mathrm{Det}[\underline{\underline{l}}^0]}{\mathrm{Det}[\underline{\underline{l}}]}\right)\right] + N\frac{F_{nem}}{k_B T} \tag{17}$$

where n_s is the number of chain strands in the network and N is the number of rods in a chain. F_{el} is the elastic free energy per strand; F_{nem}, the nematic energy per component rod of the strands. It is now important that the anisotropic step lengths characterizing the chain shape are functions of the magnitudes of nematic order Q and X as well as its orientation **n**. In the experimental geometry the free energy has to be minimized with respect to the single free strain λ_{xx} (we remind the reader that there are no shear strains in the experimental geometry presented in Figure 1 and λ_{yy} is fixed by the incompressibility constraint) and with respect to the order, characterized by Q, X, and θ. The model for the nematic PLC introduces a temperature scale $T = \upsilon\tilde{T}/k_B$ and a chain length defined in terms of the number of rods in a chain, N. The quantity N determines the relative weight of nematic to elastic free energy. The effect of altering N in subsequent calculations is purely quantitative: decreasing N increases the effect of the elastic free energy, similarly to decreasing the nematic free energy by raising the temperature. We shall take $N = 20$ where it is relevant in numerical calculations below.

There are three characteristic temperatures for a nematic rubber, the cross-linking temperature, the NI transition temperature, and the temperature at which the mechanical experiment is done. In the experiments of Mitchell, the material was cross-linked 2 deg below the NI temperature of 120 °C or, in units of T_{NI}, at $T_x = 0.995T_{NI}$. The strain was imposed at $T = 0.82T_{NI}$. In the experiments of Küpfer *et al.* the cross-linking temperature is less important, since the initial anisotropy is partly determined by the strain imposed before the second cross-linking. Their experiments were performed at a temperature of $0.94T_{NI}$.

A nematic rubber at formation has a well-defined anisotropy given by $l_\parallel^0/l_\perp^0$ in our notation. Cooling to a lower temperature spontaneously alters the shape of the rubber and its anisotropy. It was shown in earlier work[6] that this has the effect of simply redefining the initial anisotropy tensor $\underline{\underline{l}}^0$. For practical purposes we may wish to define strain with respect to this spontaneously deformed state, that is $\underline{\underline{\tilde{\lambda}}}$, whence $\underline{\underline{\lambda}} = \underline{\underline{\tilde{\lambda}}}\cdot\underline{\underline{\lambda}}_m$ where $\underline{\underline{\lambda}}_m$ is the

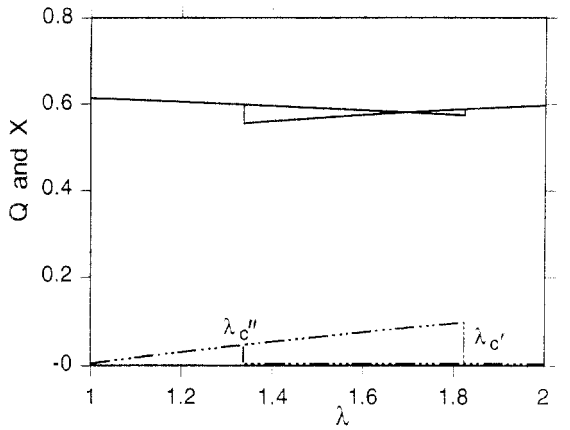

Figure 3. Variation of Q and X with applied strain λ at relatively low temperature $T = 0.9\,T_{NI}$. Strain is applied at angle $\alpha = \pi/2$ with respect to the original ordering direction. Cross-linking was carried out at a temperature $T_X \approx T_{NI}$. The order is calculated self-consistently in the freely jointed chain model. The biaxiality is small. It becomes identically zero in the state where the director has jumped to $\theta = \alpha = \pi/2$.

spontaneous deformation needed to reach the initial state. Then in (17) we have $Tr[\underline{\underline{l}}^0 \cdot \underline{\underline{\lambda}}^T \cdot \tilde{\underline{\underline{\lambda}}}^T \cdot \underline{\underline{l}}^{-1} \cdot \tilde{\underline{\underline{\lambda}}} \cdot \underline{\underline{\lambda}}_m]$. Setting instead of the initial anisotropy the effective tensor $\underline{\underline{\tilde{l}}}^0 = \underline{\underline{\lambda}}_m \cdot \underline{\underline{l}}^0 \cdot \underline{\underline{\lambda}}_m^T$, one absorbs the spontaneous deformation $\underline{\underline{\lambda}}_m$ in this definition. In what follows we shall drop the tilde sign above $\underline{\underline{\tilde{l}}}^0$ and $\tilde{\underline{\underline{\lambda}}}$ since it is precisely this anisotropic step length tensor and this strain that enter all our expressions for the mechanical conditions of the sample.

3. Results

We present in this section the results of minimizing the free energy with respect to all components θ, Q, and X of the general order parameter tensor $\underline{\underline{Q}}$ in various situations. This involves eq 3–9 that determine parameters of the elastic free energy of the nematic network, plus expressions 14 and 15 that specify the nematic free energy F_{nem}.

We investigate the effect of the changing magnitude of nematic order on the orientational transitions of a nematic rubber shown in Figure 2 for the case of constant nematic magnitude. The response of a nematic rubber to strain is significantly determined by its temperature. We will therefore investigate how lowering the temperature qualitatively affects the orientational behavior. The amount that the temperature has to be varied is dependent upon model and upon the overall weight of the nematic and elastic terms in the free energy, determined by the effective number of rods N on a chain in our system.

3.1. Cross-Link at $T \sim T_{NI}$, Strain at $T < T_{NI}$. First we look at a network formed close to its transition temperature but then strained at a lower temperature. In this case we expect that the nematic order is more rigid and the system can be approximated by an almost constant order parameter Q, as for instance has been done in earlier work.[6] We shall specifically compare those approximate results (eq 7 and 8) with the numerical calculation that takes into account the variation of Q and X during the transitions.

Lowering of the temperature causes a change in the effective step lengths in the free energy which can be calculated from the spontaneous deformation, as described above. Figure 3 shows Q and X vs λ for a melt, cross-linked at $T = 0.999T_{NI}$ and then strained at $T = 0.9T_{NI}$.

Consider for simplicity the extension axis perpendicular to the initial anisotropy direction $\mathbf{n}^0$, i.e. $\alpha = \pi/2$. As the extension λ is increased, the network becomes para-biaxial-nematic, the second-order parameter X being induced by the applied strain field. When $\lambda = 1.82$ ($\lambda_{c'}$), the phase with $\theta = 0$ becomes unstable and the director jumps to $\theta = \pi/2$, causing jumps in Q and X. It is important to emphasize that any biaxiality disappears at this point. Upon lowering λ, the state with $\theta = \pi/2$ persists until $\lambda = 1.34$ ($\lambda_{c''}$), whereupon the director rotates back to its initial orientation, θ returns to zero. These two points mark the limits to any possible hysteresis in the system. (At $\lambda = 1.52$ (λ^*) the free energies of the competing phases become equal, the point where the phase transition would occur if transitions between the two states were possible.) The rotation of the director, $\theta = \theta(\lambda)$ is qualitatively the same as has been presented in Figure 2.

That the $\theta = \pi/2$ phase should be uniaxial is somewhat surprising at first sight. It seems that the memory of cross-linking has been lost. However, the macroscopic shape remains biaxial, as can be seen from eqs 5, a signature of the original anisotropy. Meanwhile the elastic free energy at $\theta = \pi/2$ is symmetric about the $\hat{z}$ axis (the only explicit X dependence occurs in terms like $(l_1 l_2)^{-1/2}$, giving rise to positive terms in the free energy like $+X^2$). Since the nematic free energy is symmetric around the director $\mathbf{n}$, which is also aligned along the $\hat{z}$ axis, any non-zero X causes a rise in both the nematic and elastic free energy. Therefore the minimum free energy is uniaxial.

Cross-linking close to T_{NI} and performing the strain experiment at lower temperatures corresponds to the experiments of Mitchell *et al.*,[4] who cross-linked at 120 °C and strained at 50 °C at the angle $\alpha \approx \pi/2$ with respect to the initial director. This corresponds to cross-linking almost at the transition, and straining at a reduced $T = 0.82$. Under these conditions there was a drop in the order parameter at the transition of about 20%–30%, somewhat larger than the ≤10% drop predicted by the freely jointed rod model. The transition obtained by Mitchell *et al.* was softer than that predicted in Figure 2 at $\alpha = 90°$, presumably due to some small misalignment of the sample away from $\alpha = 90°$ (see Figure 2, curves b and c).

In the approximate theory, assuming the constant order parameter, the stability of the two phases has been obtained by determining when the second derivative of the free energy with respect to θ changes sign, eq 7 and 8. In the general case the free energy has a direct dependence on θ and an implicit dependence contained in Q and X, through the self-consistency conditions. We therefore have to compare the values of $\lambda_{c'}$ and $\lambda_{c''}$ obtained numerically, Figure 3, taking into account all these factors, with the constant order predictions (7). Substituting the initial value for the order parameter $Q = 0.62$ and taking $l = l^0$ in (7) we obtain $\lambda_{c'} \approx 1.77$ and $\lambda_{c''} \approx 1.33$. This compares well with the numerical data from Figure 3: $\lambda_{c'} \approx 1.82$ and $\lambda_{c''} \approx 1.34$—the correction is negligible when the transitions in orientation θ produce only small changes in Q and X. More importantly, Figure 3 shows that the assumption of constant order Q as the network is strained does not misrepresent the full theory at such low temperatures.

3.2. Strain at $\alpha \neq \pi/2$. It is possible to apply strains at some oblique angle α with respect to the initial director orientation in the sample. When $\alpha \neq \pi/2$, the curves of θ vs λ are qualitatively the same as in Figure 2. There is a region of discontinuous transitions that narrows and closes at some critical value of α to give thereafter continuous transitions. It is instructive to look at the

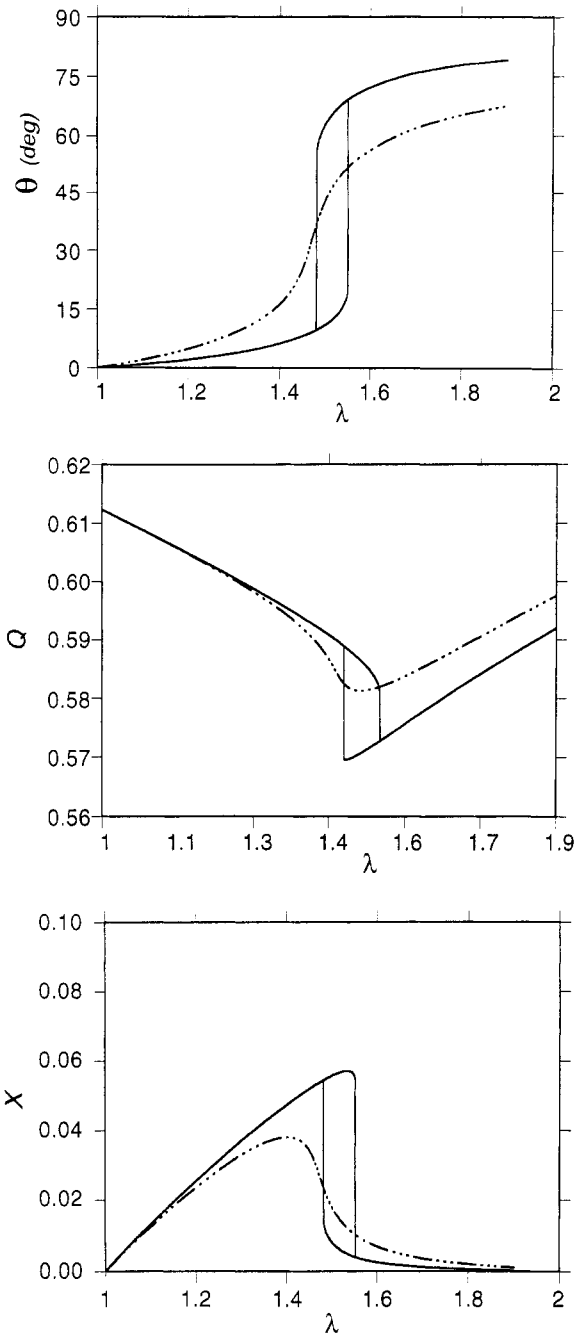

Figure 4. (a) Rotation angle θ of the director against extension λ applied at angles $\alpha = 86°$ (full line) and $\alpha = 81°$ (broken line) to the original director. This is the system of Figure 3. The discontinuous transition, with its associated hysteresis, also occurs at misalignments $\alpha \neq \pi/2$. Just as in the nonrelaxing case of Figure 2, for great enough deviations from $\alpha = \pi/2$, applied extensions no longer give rise to a discontinuous response. (b) Order parameter Q against extension λ applied at $\alpha = 86°$ (full line) and $\alpha = 81°$ (broken line). The drop in order parameter for the case of $\alpha = 86°$, though discontinuous, is not very pronounced. (c) Biaxiality X against extension λ applied at $\alpha = 86°$ (full line) and $\alpha = 81°$ (broken line). The extent of biaxiality, even at its maximum, is rather small and rapidly dies away in the high λ phase.

variation of Q and X under these conditions. Figure 4 shows the variation of θ, Q, and X with λ at $\alpha = 81°$, where the director rotates continuously toward the extension axis and $\alpha = 86°$, where the transition has become discontinuous. When $\alpha = 81°$ there is a smooth fall and then rise in the main order parameter Q; the biaxiality X rises and then falls almost to zero as $\theta \rightarrow \alpha$ (Figure 4b,c). The system adopts what is almost indistinguishable from

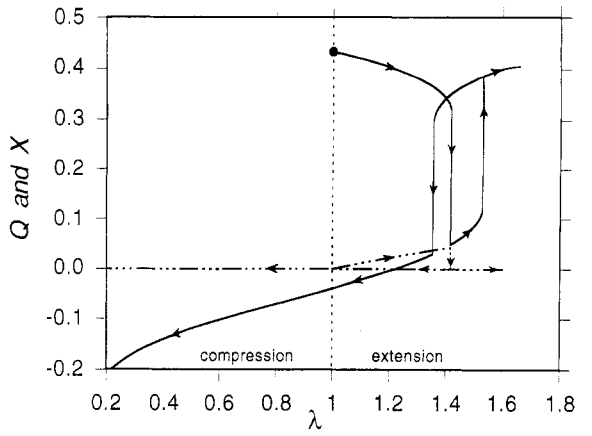

Figure 5. Order parameters Q (full line) and X (broken line) as functions of strain λ imposed at $\pi/2$ with respect to the original director. The temperature T is the same as the cross-linking temperature $T_X = 0.999T_{NI}$, that is, very close to the transition temperature. Extension starts at the heavy dot ($\lambda = 1$) and induces some small parabiaxial nematic order X while the order parameter Q decreases. There is a first transition of the director to $\theta = \alpha = \pi/2$ with a collapse of the order to a uniaxial paranematic ($X = 0$, Q low) state, followed by a second transition to a more strongly ordered uniaxial state. The direction followed by the system on increasing and then decreasing strain is indicated by the arrows. Reducing strain λ gives a hysteresis before the paranematic state with $\theta = \pi/2$ is recovered. Q becomes negative well before compression ($\lambda < 1$) is imposed, and in this model remains metastably negative down to the lowest strains ($\lambda \rightarrow 0$).

a uniaxial phase as the director becomes aligned with the strain direction.

3.3. Cross-Link and Strain at $T \sim T_{NI}$. Next we look at the case when both the cross-linking and the stretching take place close to the nematic–isotropic transition temperature at $T = 0.999T_{NI}$. In this case the nematic order is rather soft and we expect a significant order parameter variation on straining. The response to an extensional strain at $\alpha = \pi/2$ in the same experimental geometry (Figure 1) is given in Figure 5.

It is clear that the system shows a fundamentally different behavior with two transitions occurring. The nematic order is weaker than in Figures 3 and 4 of previous sections, allowing the network coupling to have a substantial influence. Increasing the strain initially introduces a para-biaxial-nematic state. At $\lambda = 1.42$ (λ_c') this biaxial state becomes unstable with respect to small variations in θ and the transition to the uniaxial state with $\theta = \pi/2$ occurs. The order is drastically reduced; in effect the system becomes para-nematic with a very low uniaxial order parameter Q. The orientational transition (the director jump from $\theta = 0$ to $\theta = \pi/2$) takes place at the same point. The equality of the free energies (the thermodynamic transition point) of these two phases occurs at $\lambda^* = 1.17$. As the strain is increased further, the material then undergoes another ordering transition to a uniaxial nematic state with much higher order, which is needed to recover the thermodynamic stability of its nematic subsystem. The limit to the stability of the para-nematic phase occurs at $\lambda = 1.53$, with the para-uniaxial/uniaxial thermodynamic transition point occurring at $\lambda = 1.44$. Naturally, this second transition and the para-nematic phase before it have no analogues in the previous analysis under assumption of a constant order parameter.

Decreasing the strain, the uniaxial phase persists until $\lambda = 1.35$ when the ordering transition to a para-nematic state occurs. The hysteresis of this transition is, therefore, from $\lambda = 1.35$ to $\lambda = 1.53$ (for our choice of $N = 20$, the number of rods per strand). However, our numerical

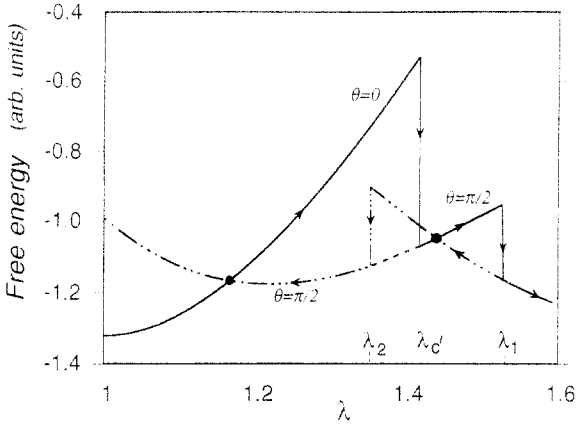

Figure 6. Free energy vs extension λ corresponding to Figure 5. The state $\theta = 0$ and the two states $\theta = \pi/2$ are labeled, as are the instabilities from $\theta = 0$ to the $\theta = \pi/2$ paranematic state ($\lambda_{c'}$), from the paranematic to nematic at $\theta = \pi/2$ (at λ_1), and from this nematic back to the paranematic (at λ_2). The thermodynamic transition points from the crossing of free energies are shown as dots. See the text for a discussion of the slopes (stresses) involved.

analysis shows that, even when the elastomer is compressed along the $\alpha = \pi/2$ axis, the paranematic state never spontaneously returns to the state with initial director orientation $\theta = 0$; *i.e.* the limit to stability point $\lambda_{c''}$ is effectively pushed to values below unity. Before the strain becomes $\lambda < 1$ (with respect to the initial state) the order parameter Q becomes negative, which reflects the fact that by reducing strain λ, one effectively compresses the rubber along its new anisotropy axis ($\theta = \pi/2$). The system becomes trapped in this metastable phase and very low uniaxial order. In practice one would have to wait for the system to "tunnel back" to the global minimum, the initial sample alignment, once strain had been released. Alternatively heating the sample above the nematic–isotropic transition temperature would recover the initial state. One can speculate on the origin of this supposed stability. The transition to the uniaxial $\theta = \pi/2$ state has been discussed in section 2. In such a state deviations (X) away from uniaxiality are energetically expensive and present a local barrier to the achievement of a state oriented along another direction (this did not obtain in the initial stage of extension where indeed $X \neq 0$ was induced). Thus the pancake state $Q < 0$ remains metastable down to unphysical values $Q = -0.5$, $\lambda \to 0$.

In Figure 6 we show the total free energy (nematic plus elastic) corresponding to Figure 5. The various points where phases become unstable are indicated, as are the thermodynamic transition points. We present this figure in order to discuss the stresses [see (10)] that must be applied in order to impose the strains specified. A positive (extensional) stress is required throughout the $\theta = 0$ state and the $\theta = \pi/2$ para-nematic state. At $\lambda = \lambda_1$ the jump to the $\theta = \pi/2$ nematic state is to a region of negative slope of F and hence a compressional stress is required to maintain $\lambda \gtrsim \lambda_1$. For long, thin samples it is possible that buckling would occur. At constant imposed extensional stress, instead of imposed strain, there would be a jump in λ to higher values where the slope is again suitably positive. To take the system back to λ_2 where there is an instability returning the system to the $\theta = \pi/2$ para-nematic state, a compressional stress must be applied. Then back on the other branch of F the slope is again positive and so again is the stress, but before $\lambda = 1$ obtains, the slope is again negative and a compressional stress would have to be applied, a necessity remaining as λ is further reduced.

The need for compressive stresses occurs in the paranematic (low Q, $\theta = \pi/2$) state even before the crossing of the $F_{\pi/2}$ and F_0 curves where it would in fact become thermodynamically advantageous to make the transition back to the $\theta = 0$ state. It is tempting to speculate whether some spatially inhomogeneous intermediate state could mediate the transition back to $\theta = 0$ once the crossing point has been passed, rather than waiting for the local instability of the homogeneous $\theta = \pi/2$ state. Imagine an intermediate state where one part of the body has an extension λ in the $\pi/2$ direction, the other part in the 0 direction. The volume of each phase is a fraction of the sample volume V. Let the interfacial width between the regions be w and the lineal dimension of the sample be S (with $S^3 = V$). The spatial dimensions of each region are $\sim\lambda S$, but in incompatible directions. There must therefore be an elastic strain between the two regions $\sim\lambda S/w$. Since $\lambda \sim 1$ we henceforth ignore it. The stored elastic strain energy is $\sim\mu S^2\omega(S/w)^2$, where μ is an elastic shear modulus for the elastomer ($\approx n_s k_B T$). The energy is $\sim\mu V(L/w)$ which clearly dictates that $w \sim S$ and that the energy of this putative intermediate is extensive in the system size. It would thus seem that fluctuations are probably an unlikely alternative to instabilities in taking the system between $\theta = 0$ and $\pi/2$.

It is interesting to note that the values for $\lambda_{c'}$ obtained numerically from Figure 5 and those estimated from the approximate (Q = const) theory (7) do not differ greatly. Substituting the initial value for the order parameter $Q = 0.43$ and taking $l = l^0$ in (7), we obtain $\lambda_{c'} \approx 1.48$, while the numerical data from Figure 5 give $\lambda_{c'} \approx 1.41$. This does not imply that the approximation works well in this region but is an artifact of the relatively small change in Q before the first transition has taken place.

The sequence of two ordering transitions with the destruction and re-forming of nematic order by the network only occurs when the coupling between the nematic and elastic parts of the free energy (via the θ dependent terms) is strong enough and the nematic order is sufficiently weak, that is, at sufficiently high temperatures.

4. Conclusions

Explicitly including a model for nematic PLC chains into the anisotropic Gaussian network description of nematic networks has enabled us to make new qualitative predictions about the ordering behavior of nematic networks under strain.

We can identify two regimes. Close to the NI transition temperature, applying strain at an angle close to 90° to the memory direction can result in the destruction of nematic order by the anisotropic elasticity. At the orientational transition the network reverts to a paranematic state, where the order is small, in some sense induced by the strain. This is followed by a purely ordering transition to a full nematic state with the director now along the strain axis. At lower temperatures the nematic order is too strong to be significantly altered by the network. The change in the order parameter is relatively small, and there is no further transition in its magnitude. In both regimes, and when $\alpha \neq \pi/2$, the system becomes uniaxial as the network anisotropy direction coincides with that of the imposed extension.

How does the existing experimental evidence support these new predictions? We can identify the experiments of Mitchell *et al.*[4] with a low-temperature transition. The nematic order is not significantly altered at the transition point. By measuring the orientation of the director θ the transition point can be unambiguously identified. The

transition is preceded by some variation of $\theta(\lambda)$ before the sharp jump in θ, probably due to some director misalignment causing the angle $\alpha \neq \pi/2$ (we have seen in Figures 2 and 4a that even a small deviation from 90° results in a dramatic change in the $\theta(\lambda)$ dependence). Mitchell *et al.*[4] also see hysteresis, the sample taking a very long time to recover its original state after releasing the strain.

The experimental evidence of Küpfer *et al.*[3] is less easy for us to interpret, due to the way in which the network was constructed. The initial cross-linking process results in a sample that would be polydomain if it were then cooled to the nematic state. Subsequent cross-linking in a strained isotropic state apparently overcomes the tendency to form polydomains and produces a monodomain, but the underlying polydomain structure may possibly reassert its influence over the network during subsequent straining, for instance forcing the sample into a scattering state. These are important questions, both theoretically and practically, for this is a useful and simple way to achieve monodomain samples.

Including a model for the nematic PLC has allowed a test of the predictions made in earlier work when the magnitude of Q was assumed to be constant. In particular, when the temperature is sufficiently low and the nematic order rigid, the transition back to the initial $\theta = 0$ orientation has been shown to be independent of Q, providing the nematic has uniaxial symmetry. At temperatures close to the isotropic phase, when the nematic order is weaker, our analysis (within the Gaussian network approximation and freely jointed rod model for the nematic) shows that the intermediate para-nematic phase with $\theta = \pi/2$ never completely loses its stability and the system may find itself trapped for a long time in these metastable conditions. The transition to $\theta = \pi/2$ at increasing strain in all cases seems to be affected only by a small amount if the coupling is weak, depending on the temperature and cross-link history. In order to test if the transitions depend significantly on temperature, new and careful experiments will need to be done and accurate estimates of the quantity λ_c made.

Acknowledgment. The authors are grateful to Peter Olmsted for many useful discussions. This work was supported by SERC U.K. (P.B. and E.M.T.) and by Unilever PLC (M.W.).

References and Notes

(1) de Gennes, P. G. *C. R. Acad. Sci.* **1975**, *B281*, 101. de Gennes, P. G. In *Polymer Liquid Crystals*; Ciferri, A., Krigbaum, W. R., Meyer, R. B., Eds.; Academic: New York, 1982. See also: Halperin, A. *J. Chem. Phys.* **1986**, *85*, 1081.
(2) Schätzle, J.; Kaufhold, W.; Finkelmann, H. *Makromol. Chem.* **1989**, *190*, 3269.
(3) Küpfer, J.; Finkelmann, H. *Makromol. Chem., Rapid Commun.* **1991**, *12*, 717.
(4) Mitchell, G. R.; Davis, F. J.; Guo, W. *Phys. Rev. Lett.* **1993**, *71*, 2947.
(5) Legge, C. H.; Davis, F. J.; Mitchell, G. R. *J. Phys. II* **1991**, *1*, 1253.
(6) Bladon, P.; Terentjev, E. M.; Warner, M. *J. Phys. II* **1994**, *4*, 75.
(7) Abramchuk, S. S.; Khokhlov, A. R. *Dokl. Akad. Nauk SSSR* **1988**, *297*, 385.
(8) Warner, M.; Gelling, K. P.; Vilgis, T. A. *J. Chem. Phys.* **1988**, *88*, 4008.
(9) Warner, M.; Wang, X. J. *Macromolecules* **1991**, *24*, 4932.
(10) Bladon, P.; Warner, M. *Macromolecules* **993**, *26*, 1078.
(11) de Gennes, P. G.; Prost, J. *The Physics of Liquid Crystals*; Clarendon: Oxford, U.K., 1993.
(12) Terentjev, E. M.; Warner, M.; Bladon, P. *J. Phys.* **1994**, *4*, 667.
(13) Warner, M.; Bladon, P.; Terentjev, E. M. *J. Phys. II* **1994**, *4*, 91.
(14) Olmsted, P. To be published in *J. Phys. II*.
(15) Golubovic, L.; Lubensky, T. C. *Phys. Rev. Lett.* **1989**, *63*, 1082.
(16) Davis, F. J.; Mitchell, G. R. *Polym. Commun.* **1987**, *28*, 8.
(17) Finkelmann, H.; Kock, H. J.; Rehage, G. *Makromol. Chem., Rapid Commun.* **1981**, *2*, 317.
(18) Canessa, G.; Reck, B.; Reckert, G.; Zentel, R. *Makromol. Chem., Macromol. Symp.* **1986**, *4*, 91.
(19) Kirste, R. G.; Ohm. H. G. *Makromol. Chem., Rapid Commun.* **1985**, *6*, 179.
(20) Mattoussi, H.; Ober, R.; Veyssie, M.; Finkelmann, H. *Europhys. Lett.* **1986**, *2*, 233.
(21) Mitchell, G. R.; Davis, F. J.; Guo, W.; Cywinski, R. *Polymer* **1991**, *32*, 1347.
(22) Rusakov, V. V.; Shliomis, M. I. *Vysokomol. Soedin., Ser. A.* **1987**, *Polym. Sci. USSR* **1987**, 29.
(23) Vasilenko, S. V.; Khokhlov, A. R.; Shibaev, V. P. *Makromol. Chem.* **1985**, *186*, 1951.
(24) Wang, X. J.; Warner, M. *J. Phys. A: Math. Gen.* **1987**, *20*, 713.
(25) Bladon, P.; Warner, M.; Liu, H. *Macromolecules* **1992**, *25*, 4329.
(26) d'Allest, J. F.; Sixou, P.; Blumstein, A.; Blumstein, R. B.; Teixeira, J.; Noirez, L. *Mol. Cryst. Liq. Cryst.* **1988**, *155*, 581.